Synthesis and gas permeation properties of chabazite-type titanosilicate membranes synthesized using nano-sized seed crystals

Sadao Araki[1]*, Hiroyasu Ishii[1], Satoshi Imasaka[1,2], Hideki Yamamoto[1]

1. Department of Chemical, Energy and Environmental Engineering, Kansai University, 3-35 Yamatecho 3-chome, Suita 564-8680, Japan

2. Functional Materials Bussiness Office, Hitachi Zosen Corporation, 2-11, Funamachi 2-Chome, Taisho-ku, Osaka 551-0021, Japan

*Corresponding author: Sadao Araki

Tel: +81-6-6368-1921

Fax: +81-6-6388-8869

E-mail: araki_sa@kansai-u.ac.jp

Abstract

Chabazite (CHA)-type zeolite membranes have received considerable attention regarding their high permeance and separation performance. A recent report detailing a unique preparation procedure for a CHA-type titanosilicate (Ti-CHA) zeolite—in which titanium heteroatoms were incorporated into the zeolite framework by substitution of aluminum—demonstrates excellent physico-chemical properties when compared with conventional aluminosilicate CHA-type zeolites. In this study, the synthesis of Ti-CHA zeolite membranes (Ti-CHA membrane) was investigated. The Ti-CHA membrane was synthesized on an alumina support *via* a secondary growth method using Ti-CHA zeolite seed crystals. The Ti-CHA membrane properties were studied as a function of seed crystal size. The average particle diameter was observed to reduce from 2.3 μm to 450 nm by increasing the loading of Ti-CHA into the synthesis gel. Regardless of the seed crystal particle size, the presence of CHA-type zeolites on the alumina support was confirmed by x-ray diffraction. UV-Vis demonstrated the incorporation of titanium heteroatoms into the zeolite framework. The results indicated the successful synthesis of the Ti-CHA membrane regardless of the seed crystal particle size. Additionally, the membrane thickness decreased by using the seed crystal. Single gas permeation tests showed that the thinnest Ti-CHA membrane prepared in this study exhibited a relatively high CO_2 permeance of $1.5\times10^{-6}\,\mathrm{mol\,m^{-2}\,s^{-1}\,Pa^{-1}}$, compared with that of previously reported CHA-type zeolite membranes. The influence of moisture on the separation performance of the Ti-CHA membrane was evaluated in the presence of gas mixtures composed of CO_2, methane and H_2O ranging from 0.1 to 5 vol.%. In the presence of 1 vol.% H_2O, the CO_2 permeance and selectivity were only marginally reduced as a result of the highly hydrophobic pore structure.

Research Highlight

・CHA-type titanosilicate zeolite membranes were prepared on α-alumina tubes.

・The membranes showed a high separation performance for CO_2/CH_4 gas mixture.

・The membrane showed high hydrophobicity.

1. Introduction

In recent years, efficient CO_2 separation technologies for natural gas and biogas refining processes have become increasingly important [1]. Separation processes based on zeolite membranes are considered as an attractive option as a result of the potential to deploy compact energy-saving devices [2]. Zeolites are crystalline materials that possess uniform pores with diameters of ≤1 nm, and thus perform as effective molecular sieves, which is a critical property in gas separation applications. However, in environments containing moisture, the hydrophilic nature of the zeolite surface, in the presence of Al, hinders the performance of zeolites in CO_2 separation applications because water selectively adsorbs within the zeolite pores, and as a result, limits zeolite-based systems from commercial exploitation [3,4]. Furthermore, as CO_2 processes are performed in high pressure environments in the presence of H_2S, there is a need to improve the physico-chemical properties of zeolites [1]. Ti silicalite-1 (TS-1) membranes, based on titanosilicate zeolites having the MFI structure, are the most common zeolite membranes in which Ti is incorporated into the zeolite framework [5,6]. TS-1 membranes exhibit superior hydrothermal stability and are utilized as ethanol selective membranes, or catalyst membranes, for liquid phase oxidation reactions in environments containing hydrogen peroxide [6].

There has recently been significant interest in chabazite (CHA)-type zeolites as materials for CO_2 separation [3,4,7]. CHA-type zeolites can be synthesized with high Si/Al molar ratios (Si/Al ratio). Zeolites having high Si/Al ratio exhibit improved physico-chemical properties and hydrophobicity. Additionally, as CHA-type zeolites possesses a three-dimensional inter-connected cage-type structure, the diffusion of guest molecules within the internal structure is expected to be enhanced. Hence, membranes

4

based on CHA-type zeolites, having eight-membered rings (0.38×0.38 nm), are considered as suitable materials for CO_2 (0.33 nm) and CH_4 (0.38 nm) separation [8–14]. We previously reported the synthesis of a Ti-CHA zeolite in which all framework Al was substituted with Ti. This substitution resulted in higher thermal and acid stability, as well as hydrophobicity, compared with conventional high-silica CHA-type zeolites (HS-CHA zeolite) and pure silica CHA-type zeolites (Si-CHA zeolite) [15].

In this study, a Ti-CHA zeolite was used as a seed crystal on a porous alumina support to grow a Ti-CHA zeolite membrane, synthesized *via* a secondary growth method. The seed crystal particle size was controlled to study the influence on the Ti-CHA membrane synthesis. The Ti-CHA zeolite seed particle size was controlled based on a seeding method [3,16]. Thereafter, Ti-CHA membranes were synthesized from Ti-CHA zeolites having various seed particle sizes. Single gas permeation tests utilizing H_2, CO_2, N_2, CH_4, and SF_6 were then conducted. Separation properties utilizing a binary CO_2/CH_4 gas mixture, in the presence or absence of moisture, were also evaluated.

2. Experiments

2.1. Preparation of Ti-CHA seed crystals

The seed crystals comprised colloidal silica (40 wt.%, Aldrich, Ludox AS-40) as the Si source, Ti oxide (TiO_2, anatase-type, Wako Pure Chemical Industries, Ltd.) as the Ti source, and *N,N,N*-trimethyl-1-adamantammonium hydroxide (TMAdaOH , 20 wt.%, SACHEM) as the structure directing agent (SDA) [15]. The colloidal silica, TiO_2, and TMAdaOH were mixed together prior to the addition of hydrofluoric acid (HF, 46 wt.%, Wako Pure Chemical Industries, Ltd.) to neutralize the solution. The mixture was then

5

heated under stirring to completely evaporate any water. The remaining product was pulverized with an agate mortar and pestle. Thereafter, water was added to prepare a synthetic gel. The molar composition of the gel was: $1.0 \, SiO_2$: $0.033 \, TiO_2$: 1.4 TMAdaOH: $1.4 \, HF$: $6.0 \, H_2O$ (Si/Ti = 30). The prepared gel was transferred to an autoclave and hydrothermally treated in an oven at 423 K for 24 h. Thereafter, the autoclave was removed from the oven and cooled, the product was filtered and washed with ion-exchanged water before drying under reduced pressure for 24 h to obtain Ti-CHA zeolite seed particles (CTS-0). To decrease the particle size, Ti-CHA zeolite seed particles (1.6–10 wt.%, based on total SiO_2) was added to the synthetic gel with the molar composition of $1.0 \, SiO_2$: $0.033 \, TiO_2$: $1.4 \, TMAdaOH$: $1.4 \, HF$: $6.0 \, H_2O$. The subsequent procedures were the same as CTS-0.

2.2. Fabrication of Ti-CHA zeolite membranes

Ti-CHA membranes were synthesized *via* a secondary growth method comprising seed crystals deposited on the surface of an alumina support. A synthetic gel was prepared as per the Ti-CHA zeolite procedure. The molar composition of the gel was: $1.0 \, SiO_2$: 0.033 TiO_2: $1.4 \, TMAdaOH$: $1.4 \, HF$: $6.0 \, H_2O$ (Si/Ti = 30). Ti-CHA zeolite powders, having varying seed particle sizes were coated onto the outer surface of an α-alumina porous support *via* a rubbing method (outer diameter: 16 mm, length: 40 mm, average pore diameter: 0.5–1.0 μm, Hitachi Zosen Corp.). The synthesized gel was then put onto the support coated with seed crystals, and the entire support surface was rapped with polytetrafluoroethylene tape. The samples were transferred to an autoclave and subjected to hydrothermal synthesis at 423 K for 72 h. Thereafter, the samples were washed with water and then dried under reduced pressure for 24 h. Finally, the samples were calcined

in a furnace at 853 K for 12 h to remove the TMAdaOH to obtain the final Ti-CHA membranes.

2.3. Characterization

X-ray diffraction (XRD, Rigaku, Ultima-IV) was used for phase identification of the Ti-CHA zeolites and Ti-CHA membranes. Particle size, thickness and morphology of the zeolite layers were observed by field emission scanning electron microscopy (FE-SEM, Hitachi High-Technologies, HITACHI S-4800). The chemical bonding states of the Ti species in the zeolite framework were analyzed *via* UV-Vis spectroscopy (JASCO corporation, V-550). The UV-Vis spectra were obtained from mixtures with magnesium oxide as a reference substance. The chemical composition of the zeolites was measured by inductively coupled plasma-optical emission spectroscopy (ICP-OES, Shimadzu Corporation, ICPS-7510). ICP-OES measurements were performed on the Ti-CHA zeolite (0.01 g), which was dissolved in a mixture of ion-exchanged water (20 g) and HF (5 ml). Regarding the membranes, the powder that was scraped off the surface with sandpaper was analyzed *via* ICP-OES and UV-Vis spectroscopy. To calculate the specific surface area and micropore volume of each zeolite, nitrogen adsorption measurements (MicrotracBEL corporation, BELSORP-mini II) were performed. Specific surface areas were calculated based on the Brunauer-Emmett-Teller (BET) model and micropore volumes were calculated based on the t-plot model [17].

2.4. Single gas permeance and CO_2/CH_4 gas mixture separation tests

The single gas permeance for H_2, CO_2, N_2, CH_4, and SF_6, diffused through Ti-CHA membranes, was evaluated using the equipment presented in Fig. 1. After the membrane

was placed into a module, each gas was fed to the outer side of the membrane, with N_2

being fed to the inner side of the support as a sweep gas. The pressure inside the support

was fixed at standard atmospheric pressure, while the outside of the membrane was

pressurized using a back-pressure regulator to create a pressure difference across the

membrane of 0.1 MPa. Over a temperature range of 313–433 K, the flow rates of the

permeated gases were measured using a soap film flow meter, and their respective

concentrations measured by GC (GC-8A, Shimazu, Japan). Single gas permeance (mol

$m^2 \, s^{-1} \, Pa^{-1}$) was calculated by dividing the obtained permeation flux (mol $m^{-2} \, s^{-1}$) by the

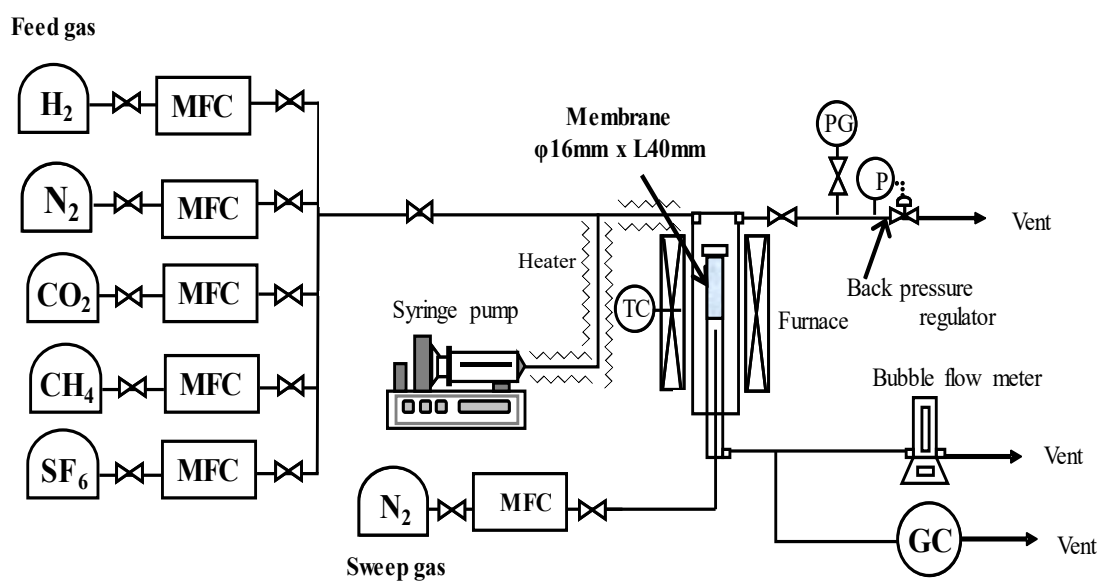partial pressure difference across the membrane.

Fig. 1. Schematic diagram of experimental apparatus.

The separation properties of the Ti-CHA membrane, for a binary CO_2/CH_4 gas mixture,

were also evaluated. The N_2 sweep gas was fed into the inside of the support and the

pressure difference across the membrane was 0.1 MPa. After CO_2/CH_4 equimolar gas

mixtures were introduced, using a mass flow controller, the flow rates of the gas

8

permeation, at temperatures of 313–433 K, were measured using the soap film flow meter, and the concentrations of CO_2 and CH_4 were analyzed by GC. The permeance values for each gas and the selectivity (-), which is the ratio of the permeance of CO_2 to that of CH_4, were calculated to evaluate separation performance. Furthermore, the influence of moisture (up to 5 vol.%) on the separation of the binary CO_2/CH_4 gas mixture by the Ti-CHA membrane was investigated, at 313 K. The deionized water was fed by the syringe pump and then vaporized by heater.

3. Results and discussion

3.1. Ti-CHA zeolite seed crystals: size control and properties

Table 1 summarizes the Si/Ti ratios, BET specific surface areas, and micropore volumes of the seed crystal particles, prepared by adding the Ti-CHA zeolite to the synthetic gel. ICP-OES data show the Si/Ti ratios of the seed crystals to be in the range of 234–587, however, there is no trend of Si/Ti ratio as a function of the amount of zeolite added to the synthetic gel. Further studies are needed to clarify this phenomenon. However, the existence of titanium on the zeolite particle was confirmed from this result. Similarly, the BET specific surface areas were also unaffected by the amount of zeolite added. In comparison with the CHA-type titanosilicate seed-0 (CTS-0), to which no zeolite was added, the micropore volumes were slightly reduced in the Ti-CHA seed crystals prepared by the seeding method (CTS-1, 2, 3 and 4). The XRD patterns of the seed crystal particles are presented in Fig. 2. Although small differences in their peak intensities were observed, the CHA structure was obtained as a pure phase for all seed crystals, confirming the formation of the Ti-CHA zeolite. CTS-0 showed a higher peak

intensity compared with the Ti-CHA zeolites (CTS-1, 2, 3, 4). This reduction of intensity for the Ti-CHA zeolites was as a result of the reduced crystallite size induced by the seeding method.   Jhang *et al.* prepared Si-CHA zeolites using the seeding method and the peak intensity for Si-CHA zeolites decreased with increasing the seed contents [16].

Table 1 Physico-chemical properties of various CHA-type zeolites.

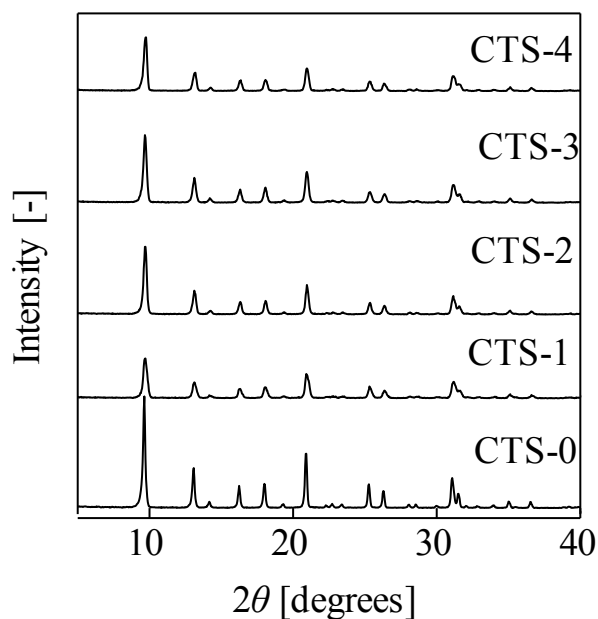| Sample	Synthesis gel	Product		
	Added amount of Ti-CHA zeolite [wt.%]	Si/Ti	S_{BET} [m^2 g^{-1}]	V_{micro} [cm^3 g^{-1}]
CTS-0	0	347	813	0.295
CTS-1	1.6	234	755	0.268
CTS-2	2.8	587	770	0.274
CTS-3	5.2	394	823	0.269
CTS-4	10	425	758	0.271

Fig. 2. XRD patterns of Ti- CHA zeolite seed crystals.

FE-SEM images of the Ti-CHA zeolites are presented in Fig. 3. Cube-like morphology is observed, which is characteristic of CHA-type zeolites. While the particle size of CTS-

0 was observed to be on the order of micrometers, the other samples exhibited particle sizes on the order of nanometers. Hence, by adopting the seeding method, the Ti-CHA zeolite particle size could be significantly reduced. Furthermore, the average particle size decreased as a function of increased zeolite content added to the synthesis gel, as shown in Fig. 4. The values of standard error (N=100) of CST-0, 1, 2, 3 and 4 were 52 nm, 16 nm, 14 nm, 11 nm and 12 nm, respectively. The average particle size of CTS-1, 2, 3, and 4 was observed to be 748 nm, 624 nm, 555 nm, and 455 nm, respectively. This phenomenon can be attributed to the increased number of nuclei for the formation of zeolite crystals as a result of the increased zeolite loading. The zeolite added to the synthesis gel was previously broken down by HF, and various intermediates that act as the nuclei for the Ti-CHA zeolite were also formed. A large number of nuclei present in the system restricts particle size growth. By adopting the seeding method, the average Ti-CHA zeolite particle size could be tailored within the range of several μm to 450 nm.
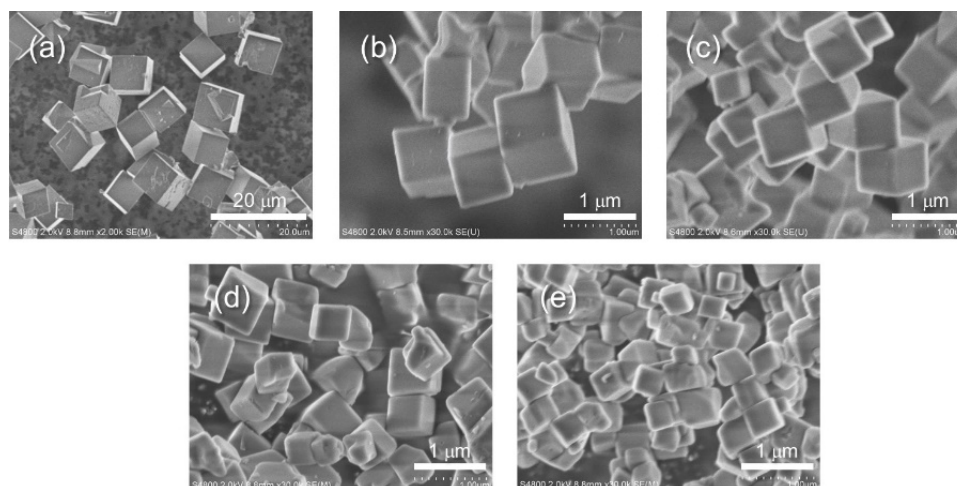

Fig. 3. FE-SEM images of Ti-CHA zeolite seed crystals; (a) CTS-0, (b) CTS-1, (c) CTS-2, (d) CTS-3 and (e) CTS-4.
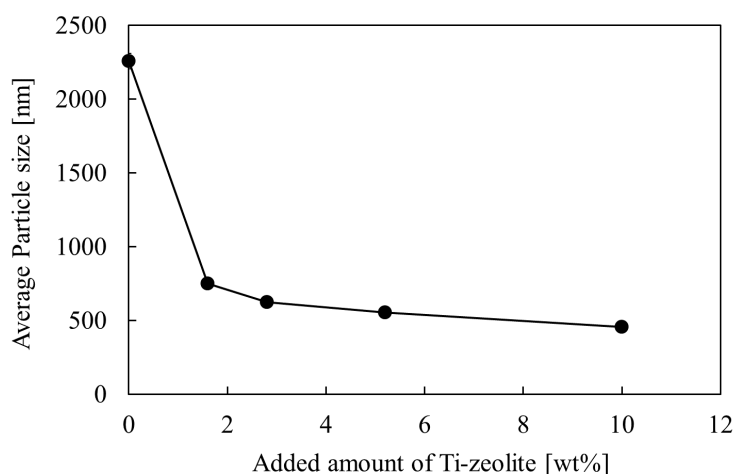
Fig. 4. Particle size as a function of Ti-CHA zeolite content added to the synthesis gel.

3.2. Ti-CHA membrane morphology

Ti-CHA membranes, termed CTM-0, CTM-1, CTM-2 and CTM-3, were prepared in the presence of the Ti-CHA zeolite seed crystals of CTS-0, CTS-1, CTS-2 and CTS-3, respectively. The synthesis conditions for each of the Ti-CHA membranes are listed in Table 2. The Si/Ti ratios of the prepared zeolite membranes vary across the range of 152–287. Basically, the Si/Ti ratio should be constant when the Si/Ti ratio of seed crystal, gel composition and hydrothermal condition were same. No correlation was observed between the Si/Ti ratio of the membrane and the particle size of the seed crystal. However, the existence of titanium on the surface zeolite layer was confirmed from this result.

Table 2 Ti-CHA membrane synthesis conditions and Si/Ti ratios of the prepared membranes.

| Membrane | Ti-CHA zeolite seed crystal | | Prepared membrane |
	Sample No.	Average particle size [μm]	Si/Ti ratio
CTM-0	CTS-0	6.0	172
CTM-1	CTS-1	0.75	155
CTM-2	CTS-2	0.62	287
CTM-3	CTS-3	0.55	276

12

The XRD patterns of the prepared zeolite membranes are presented in Fig. 5. Peaks for all membrane samples were observed at $2\theta = 9.4°$, $20.5°$, and $30.4°$, which correspond to the (1 0 0), (2 0 −1), and (3 −1 −1) planes of the CHA zeolite. Furthermore, peaks attributed to the α-alumina supports were also detected at approximately $2\theta = 35.2°$ and $37.9°$. These results suggest that CHA-type zeolite layers were formed on the outer surfaces of the α-alumina supports. There were no significant differences in peak intensities between different membranes. However, for the Ti-CHA membranes prepared using nano-sized seed crystals (CTM-1, CTM-2 and CTM-3) the nano-sized seed, the unidentifiable tiny peak was observed at about 5°, which is not derived from any type of titanium oxide and FAU zeolite as the precursor.
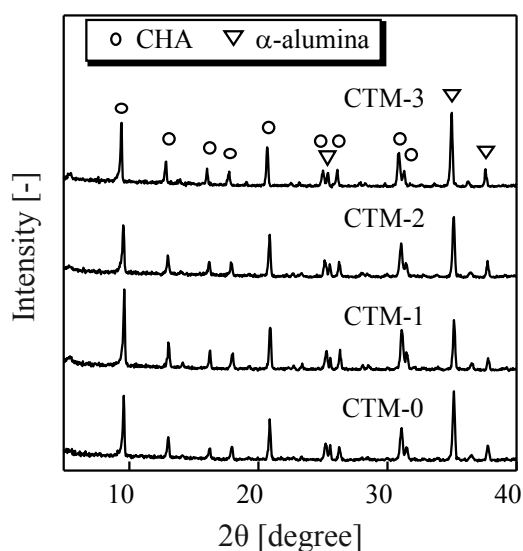

Fig. 5. XRD patterns of Ti-CHA membranes.

The chemical states of the Ti species within the framework of the Ti-CHA membrane were analyzed by UV-Vis spectroscopy (Fig. 6). Peaks at 220 nm, which are attributed to isolated tetrahedral-coordinated Ti species, were detected for all Ti-CHA membranes [18,19]. This result demonstrates the successful incorporation of Ti into the zeolite

framework. Additional peaks were detected at approximately 260–280 nm for all Ti-CHA membranes, which correspond to octahedral-coordinated extra-framework Ti species that are not incorporated into the zeolite framework [18,19].
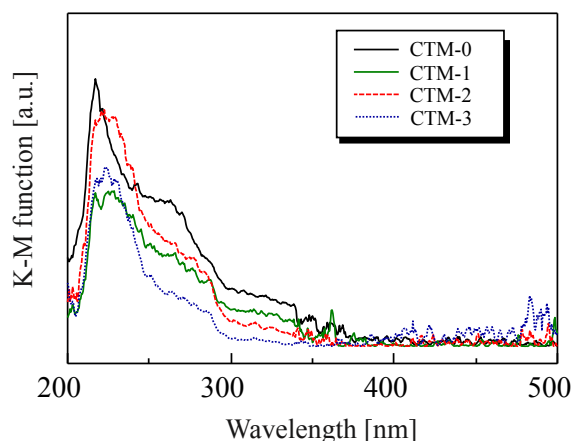

Fig. 6. UV-vis spectra of Ti-CHA membranes

Fig. 7 shows FE-SEM images of the surface morphologies and cross sections of the Ti-CHA membranes. Cube-like crystal particles that are typical of CHA-type zeolites, that comprised microscopic particles, were observed in all membrane surfaces. The polycrystalline layer formation is considered as a result of the secondary growth of the seed crystals [3]. Therefore, differences in the surface structure of the membranes were observed according to the size of the seed crystals utilized. A high degree of particles was deposited onto the CTM-0 membrane surface prepared using micro-sized seed crystals (CTS-0), and interstitial voids were observed. Conversely, the Ti-CHA membranes prepared using nano-sized seed crystals (CTM-1, CTM-2 and CTM-3), were completely covered by crystal particles with no interstitial voids observed. Furthermore, the thicknesses of the zeolite layers for the Ti-CHA membranes prepared using nano-sized seed crystals obviously reduced to about 10 μm, from about 20 μm for the CTM-0 membrane. However, a significant difference for the thickness of the zeolite layer among

14

the Ti-CHA membranes prepared using nano-sized seed crystals was not observed by FE-SEM.
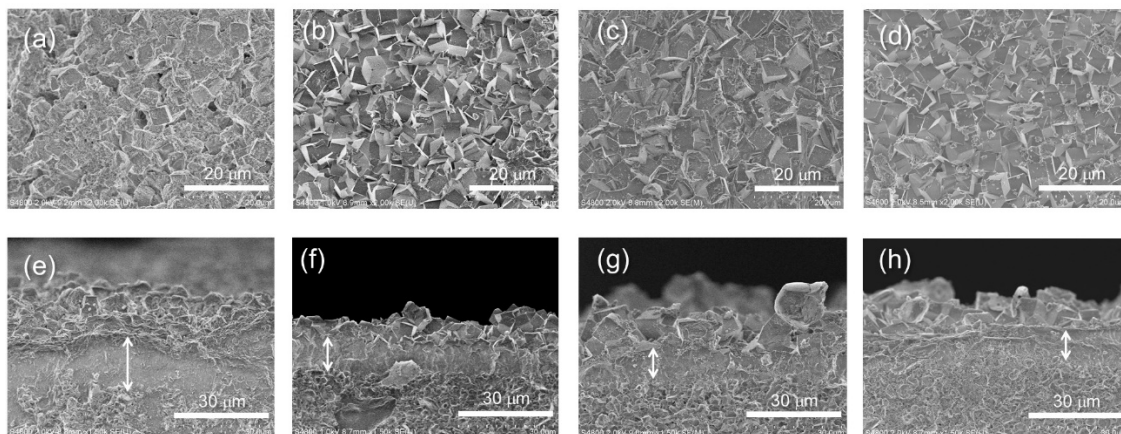

Fig. 7. FE-SEM images of Ti-CHA membranes: (a) surface of CTM-0, (b) surface of CTM-1, (c) surface of CTM-2, (d) surface of CTM-3, (e) cross-section through CTM-0, (f) cross-section through CTM-1, (g) cross-section through CTM-2 and (g) cross-section through CTM-3.

3.3. Single gas permeance and CO_2/CH_4 gas separation performance

Single gas permeance tests for H_2, CO_2, N_2, CH_4, and SF_6, conducted over CTM-0 and CTM-2 membranes, were evaluated. Fig. 8 shows the gas permeance, at 313 K, for each gas as a function of kinetic diameter. All permeance for the CTM-2 membrane was higher than that of the CTM-0 membrane. Particularly, the CO_2 permeance for the CTM-2 membrane was reached at 1.5×10^{-6} mol m^{-2} s^{-1} Pa^{-1}. It is considered that this result is due the reduced zeolite layer as shown in Fig 7.

For both Ti-CHA membranes, the permeance values significantly reduced at a kinetic diameter of 0.38 nm (CH_4), which is also the same value as the pore size of the CHA-type zeolite. This phenomenon is the result of molecular sieving. For both membranes,

15

CO_2 permeance paradoxically exhibited the highest values among the measured gases. In other words, higher permeance values were observed when compared with H_2, whose kinetic diameter is smaller than that of CO_2. Therefore, it is expected that the permeance of H_2 should be higher than that of CO_2. This phenomenon was observed in the case of HS-CHA membrane at 298 K [12] and Si-CHA membrane at 313 K [3]. The CO_2 permeance is promoted by the affinity between the partial charges on the CO_2 molecules and the polarity of the zeolites [20].

Fig. 9 shows the effect of the diameter of seed crystal on the CO_2 permeance and the ideal selectivity, which is permeance ratios, for the gas mixtures. The CO_2 permeance increased with decreasing the diameter of the seed crystal. This might be due to a decrease in zeolite layer, which couldn't be observed by FE-SEM, as shown in Fig. 7. All ideal selectivity for all membranes were larger than those calculated based on Knudsen diffusion (CO_2/N_2: 0.6, CO_2/CH_4: 0.8 and CO_2/SF_6: 1.8). Here, the membranes are assumed to be free of any significant defects such as pinholes or cracks. The ideal selectivity values showed a slight tendency to increase with decreasing the diameter of the seed crystal. However, in the case of the CTM-3 membrane, the permeance ratios decreased compared with the CTM-2 membrane. The thinner thickness of the zeolite layer increases the probability of the creation of pinholes or cracks. In addition, SF_6 permeance of Si-CHA membrane, which shows similar CO_2 permeance (1.7×10^{-6} mol m^{-2} s^{-1} Pa^{-1}) with Ti-CHA membrane, is 4-5 $\times 10^{-9}$ mol m^{-2} s^{-1} Pa^{-1} at 313 K and is smaller than that of Ti-CHA membranes. At this moment, the CTM-2 membrane was observed to exhibit the highest permeance ratios for and formed a highly dense zeolite layer.
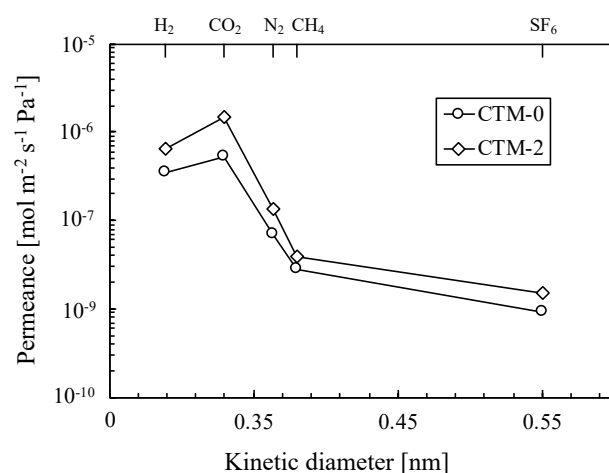
16

Fig. 8. Single gas permeance values of Ti-CHA membranes at a differential pressure of 0.1 MPa and temperature of 313 K.
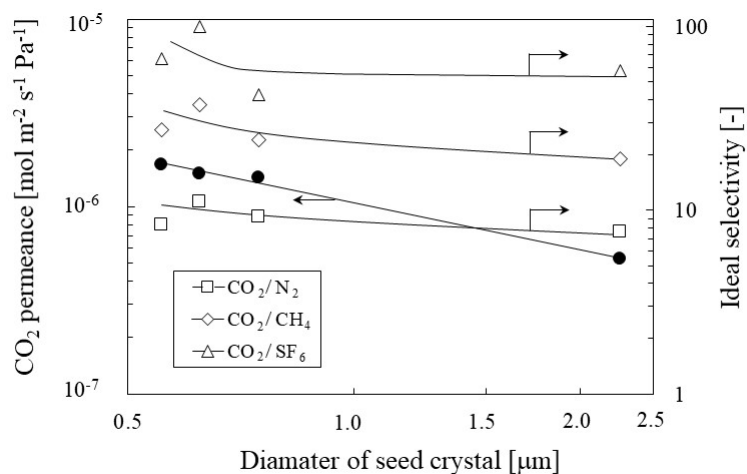

Fig. 9 Relationship between diameter of seed crystal and permeation properties.

Table 3 Comparison of CO_2 permeance and ideal selectivity with other CHA-type membranes.

Membrane	Temperature [K]	Support	Differential pressure [MPa]	CO_2 permeance $[10^{-7}\,mol\,m^{-2}\,s^{-1}\,Pa^{-1}]$	Ideal selectivity [-]	Ref.
HS-CHA	303	α-alumina disk	0.1	0.34	22	10
	303	Mullite tube	0.2[a]	3	360	11
	298	Stainless-steel tube	0.138	1.6	11	12
	293	Mullite tube	0.08	2.1±0.14	110±34	13
	Room temp.	α-alumina disk	0.45	121	50	14
Si-CHA	313	α-alumina tube	0.1	17	54	3
	313	α-alumina tube	0.1	41	74	4
SAPO-34[b]	298	α-alumina hollow fiber	0.1	11.8	160	21
Ti-CHA	313	α-alumina tube	0.1	15	38	This study

[a] Feed pressure, [b] separation performance of binary

Table 3 lists the single CO_2 permeance and the ideal selectivity of other CHA-type membranes (HS-CHA, Si-CHA, SAPO-34). The Ti-CHA membrane showed a relatively high single CO_2 permeance with the relatively high ideal selectivity [3,4,10–14,21].

The separation of a binary CO_2/CH_4 gas mixture was evaluated utilizing CTM-2. Fig. 10 shows the temperature dependence of the CO_2 and CH_4 permeance and selectivity values in single and binary gas systems. For both the single and binary gas systems, the permeance values for CO_2 decreased with increasing testing temperature above 313 K. Conversely, the permeance values of CH_4 were temperature-independent and almost constant, resulting in decreased selectivity values at higher temperatures. Although the permeance of CO_2 is promoted by adsorption onto CHA-type zeolites, this effect is thought to be reduced under high-temperature conditions [10]. The CH_4 permeance values in the binary gas system were observed to decrease when compared with the corresponding single gas system. The decrease of CO_2 permeance was smaller than that of CH_4 permeance. As a result, the selectivity values were observed to be higher in the binary gas system, which can be attributed to the selective adsorption of CO_2, preferentially located on the membrane surface and within the zeolite pores. Therefore, the CH_4 molecules were blocked by the CO_2 molecules, thereby inhibiting adsorption and reducing the permeance values.
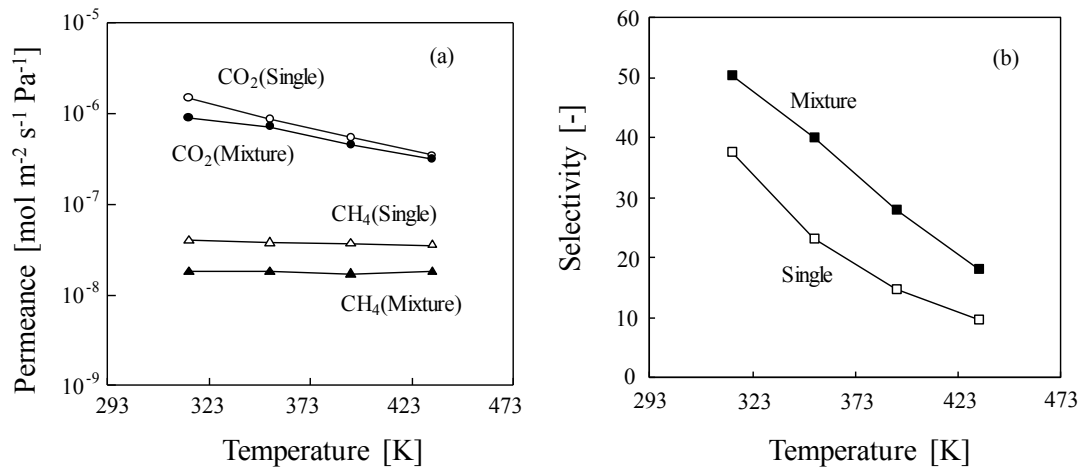
18

Fig. 10. Influence of feed temperature on the equimolar CO_2/CH_4 separation with the CTM-70 membrane at a differential pressure of 0.1 MPa. (a) Permeance. (b) Selectivity.

The influence of moisture concentration on the separation performance of CTM-2 for a binary equimolar CO_2/CH_4 gas mixture was also evaluated, at 313 K. Fig. 11 presents the reduction rates of the CO_2 permeance and selectivity values relative to the water concentration in the feed gas. With increasing water content in the feed gas mixture, the permeance and CO_2 selectivity were not observed to decrease for the Ti-CHA membrane, even with the addition of 0.1 vol.% moisture. Furthermore, increasing the moisture content to 1 vol.%, CO_2 permeance remained at 80%, while CO_2 selectivity was maintained at ~100%. When further increasing the water vapor concentration to 5 vol.%, the selectivity was maintained at ≥70%. In the presence of 0.6 vol.% of water vapor, the CO_2 permeance of the SAPO-34 membrane decreases from ~1.0×10^{-7} mol m^{-2} s^{-1} Pa^{-1} to 8.0×10^{-10} mol m^{-2} s^{-1} Pa^{-1} [22]. Furthermore, Kida $et\ al.$ evaluated the influence of moisture on the separation performance of Si-CHA membrane for the binary equimolar CO_2/CH_4 gas mixture [4]. Under humidified conditions with saturated steam (about 1.6 vol. %) at 298 K and difference pressure of 0.1 MPa, the CO_2 permeance drastically

19

decreased to about the one-hundredth value and the selectivity decreased by more than 90 % from 130 to 10. These differences might arise depending on the hydrophilic or hydrophobic nature of the membrane, however we can't completely arrive at this conclusion due to the experimental difference about H_2O concentration and temperature. However, the Ti-CHA zeolite has a relatively high hydrophobic nature compared with the aluminosilicate CHA zeolite and the pure silica CHA zeolite due to the small number of silanol groups [15]. Hence, it is considered that the results derive from the highly hydrophobic nature of the pores.
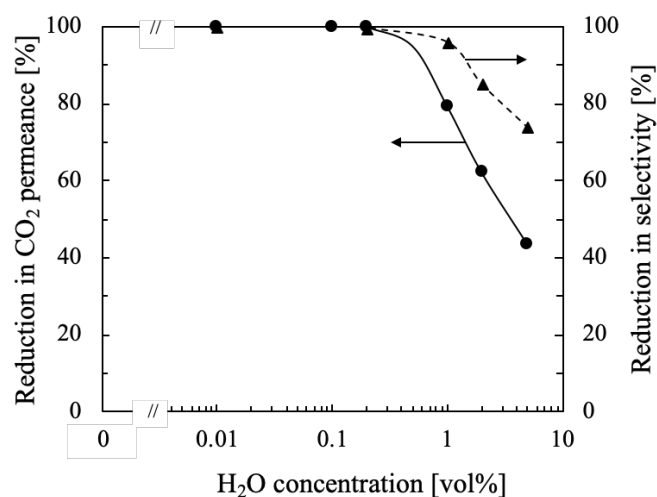

Fig. 11 Influence of H_2O concentration on the equimolar CO_2/CH_4 separation at a temperature of 313 K and differential pressure of 0.1 MPa.

4. Conclusions

In this study, Ti-CHA membranes were synthesized on α-alumina supports *via* the secondary growth of Ti-CHA zeolite seed crystals. The Ti-CHA zeolite particle size was controlled from several μm down to 450 nm by controlling the loading level of the Ti-CHA crystals in the synthesis gel. The Ti-CHA membranes prepared using nanoscale

seed crystals demonstrated excellent CO_2 permeance, even in the presence of a binary CO_2/CH_4 gas mixture. Furthermore, the influence of moisture on the CO_2/CH_4 separation performance, for the Ti-CHA membranes, was confirmed to be relatively small. These results indicate that Ti-CHA membranes are promising materials for CO_2 gas separation applications in natural gas and biogas refining processes.

References

[1] N. Kosinov, J. Gascon, F. Kapteijn, E. J. M. Hensen, Recent developments in zeolite membranes for gas separation, *J. Membr. Sci.* 499 (2016) 65–79.

[2] T. Tomita, K. Nakayama, H. Sakai, Gas separation characteristics of DDR type zeolite membrane, *Micropor. Mesopor. Mater.* 68 (2004) 71–75.

[3] K. Kida, Y. Maeta, K. Yogo, Preparation and gas permeation properties on pure silica CHA-type zeolite membranes, *J. Membr. Sci.* 522 (2017) 363–370.

[4] K. Kida, Y. Maeta, K. Yogo, Pure silica CHA-type zeolite membranes for dry and humidified CO_2/CH_4 mixtures separation, *Sep. Purif. Technol.* 197 (2018) 116–121.

[5] X. Chen, P. Chen, H. Kita, Pervaporation through TS-1 membrane, *Micropor. Mesopor. Mater.* 115 (2008) 164–169.

[6] P. Chen, X. Chen, X. Chen, H. Kita, Preparation and catalytic activity of titanium silicalite-1 zeolite membrane with TPABr as template, *J. Membr. Sci.* 330 (2009) 369–378.

[7] M. Miyamoto, Y. Fujiokax. K. Yogo, Pure silica CHA type zeolite for CO_2 separation using pressure swing adsorption at high pressure, *J. Mater. Chem.* 22 (2012) 20186–20189.

[8] S. Imasaka, M. Itakura, K. Yano, S. Fujita, M. Okada, Y. Hasegawa, C. Abe, S. Araki, H. Yamamoto, Rapid preparation of high-silica CHA-type zeolite membranes and their separation properties, *Sep. Purif. Technol.* 199 (2018) 298–303.

[9] N. Kosinov, C. Auffret, C. G¨uc¨uyener, B. M. Szyja, J. Gascon, F.Kapteijn, E. J. M. Hensen, High flux high-silica SSZ-13 membrane for CO_2 Separation, *J. Mater. Chem. A.* 2 (2014) 13083–13092.

[10] H. Maghsoudi, M. Soltanieh, Simultaneous separation of H_2S and CO_2 from CH_4 by a high silica CHA-type zeolite membrane, *J. Membr. Sci.* 470 (2014) 159–165.

[11] Y. Zheng, N. Hu, H. Wang, N. Bu, F. Zhang, R. Zhou, Preparation of steam-stable high-silica CHA(SSZ-13) membranes for CO_2/CH_4 and C_2H_4/C_2H_6 separation, *J. Membr. Sci.* 475 (2015) 303–310.

[12] H. Kalipcilar, T. C. Bowen, R. D. Noble, J. L. Falconer, Synthesis and Separation Performance of SSZ-13 Zeolite Membranes on Tubular Supports, *Chem. Mater.* 14 (2002) 3458–3464.

[13] T. Wu, M. C. Diaz, Y. Zheng, R. Zhou, H. H. Funke, J. L. Falconer,

R. D. Noble, Influence of propane on CO_2/CH_4 and N_2/CH_4 separations in CHA zeolite membranes, *J. Membr. Sci.* 473 (2015) 201–209.

[14] L. Yu, A. Holmgren, M. Zhou, J. Hedlund, Highly permeable CHA membrane prepared by fluoride synthesis for efficient CO_2/CH_4 separation, *J. Mater. Chem. A*, 6 (2018) 6847–6853.

[15] S. Imasaka, H. Ishii, J. Hayashi, S. Araki, H. Yamamoto, Synthesis of CHA-type titanosilicate zeolites using titanium oxide as Ti source and evaluation of their physicochemical properties, *Micropor. Mesopor. Mater.* 273 (2019) 243–248.

[16] J. Zhang, X. Liu, M. Li, C. Liu, D. Hu, G. Zeng, Y. Zhang, Y. Sun, Fast synthesis of submicron all-silica CHA zeolite particles using a seeding method, *RSC Adv*, 5 (2015) 27087–27090.

[17] Q. Zhu, J. N. Kondo, R. Ohnuma, Y. Kubota, M. Yamaguchi, T. Tatsumi, The study of methanol-to-olefin over proton type aluminosilicate CHA zeolites, *Micropor. Mesopor. Mater.* 112 (2008) 153–161.

[18] M. Tamura, W. Chaikittisilp, T. Yokoi, T. Okubo, Incorporation process of Ti species into the framework of MFI type zeolite, *Micropor. Mesopor. Mater.* 112 (2008) 202–210.

[19] Y. Kunitake, T. Takata, Y. Yamasaki, N. Yamanaka, N. Tsunoji, Y. Takamitsu, M. Sadakane, T. Sano, Synthesis of titanated chabazite with enhanced thermal stability by hydrothermal conversion of titanated faujasite, *Micropor. Mesopor. Mater.* 215 (2015) 58–66.

[20] P. Bai, M. Tsapatsis, J. I. Siepmann, TraPPE-zeo: Transferable Potentials for Phase Equilibria Force Field for All-Silica Zeolites, *J. Phys. Chem. C.* 117 (2013) 23475–24387.

[21] Y. Chen, Y. Zhang, C. Zhang, J. Jiang, X. Gu, Fabrication of high-flux SAPO-34

membrane on α-Al2O3 four-channel hollow fibers for CO_2 capture from CH_4, *J. CO2 Util.* 18 (2017) 30–40.

[22] J. C. Poshusta, R. D. Noble, J. L. Falconer, Characterization of SAPO-34 membranes by water adsorption, *J. Membr. Sci.* 186 (2001) 25–40

Figure legends

Fig. 1 Schematic diagram of experimental apparatus.

Fig. 2 XRD patterns of Ti- CHA zeolite seed crystals.

Fig. 3 FE-SEM images of Ti-CHA zeolite seed crystals; (a) CTS-0, (b) CTS-1, (c) CTS-2, (d) CTS-3 and (e) CTS-4.

Fig. 4 Particle size as a function of Ti-CHA zeolite content added to the synthesis gel.

Fig. 5 XRD patterns of Ti-CHA membranes.

Fig. 6 UV-vis spectra of Ti-CHA membranes.

Fig. 7 FE-SEM images of Ti-CHA membranes: (a) surface of CTM-0, (b) surface of CTM-1, (c) surface of CTM-2, (d) surface of CTM-3, (e) cross-section through CTM-0, (f) cross-section through CTM-1, (g) cross-section through CTM-2 and (g) cross-section through CTM-3.

Fig. 8 Single gas permeance values of Ti-CHA membranes at a differential pressure of 0.1 MPa and temperature of 313 K.

Fig. 9 Relationship between diameter of seed crystal and permeation properties.

Fig. 10 Influence of feed temperature on the equimolar CO2/CH4 separation with the CTM-2 membrane at a differential pressure of 0.1 MPa. (a) Permeance. (b) Selectivity.

Fig. 10. Influence of H_2O concentration on the equimolar CO_2/CH_4 separation at a temperature of 313 K and differential pressure of 0.1 MPa.

Table legends

Table 1 Physico-chemical properties of various CHA-type zeolites.

Table 2 Ti-CHA membrane synthesis conditions and Si/Ti ratios of the prepared membranes.

Table 3 Comparison of CO_2 permeance and ideal selectivity with other CHA-type membranes.